Cureus
Part of SPRINGER NATURE

Open Access Review Article

Stromal and Regulatory T Cell Circuits in the Tumor Microenvironment and Their Therapeutic Implications: A Narrative Review

Review began 10/29/2026
Review ended 11/09/2026
Published 11/14/2026

© **Copyright** 2026
Pan et al. This is an open access article distributed under the terms of the Creative Commons Attribution License CC-BY 4.0., which permits unrestricted use, distribution, and reproduction in any medium, provided the original author and source are credited.

DOI: 10.7759/cureus.119651

Yang Pan [1], Tao Lu [1], Jiajie Wang [1], Bingbing Lu [1], Xixian Ke [1], Junliang Ma [1]

1. Department of Thoracic Surgery, Zunyi Medical University Affiliated Hospital, Zunyi, CHN

Corresponding author: Junliang Ma, xwkmjl123@zmu.edu.cn

Abstract

Regulatory T cells (Tregs) and stromal cells jointly shape immune suppression in tumors. This narrative review examines Treg interactions with cancer-associated fibroblasts, blood and lymphatic endothelial cells, adipocytes, and mesenchymal stromal cells. Four processes connect these compartments: spatial positioning, functional programming, metabolic conditioning, and reciprocal remodeling.

Fibroblast-derived chemokines and antigen presentation influence Treg localization and activity, endothelial barriers alter lymphocyte access and survival, and metabolic signals support local immune adaptation. Treg-derived mediators, in turn, reshape stromal behavior. Cellular origin, stromal state, and tissue context determine how these interactions affect antitumor immunity.

Clinical studies distinguish target-associated immune changes from treatment benefit. These findings favor therapeutic selection based on the specific stromal-Treg interaction operating in a tumor rather than stromal abundance alone. Combining cellular and spatial biomarkers with paired-tissue pharmacodynamic assessment can connect the proposed mechanism of treatment to its clinical effects.

Categories: Oncology, Allergy/Immunology
Keywords: cancer-associated fibroblasts, immunotherapy, regulatory t cells, stromal cells, tumor microenvironment

Introduction And Background

Tumor behavior reflects interactions among malignant cells, immune cells, stroma, extracellular matrix and metabolites that influence growth, invasion and treatment response [1]. Regulatory T cells (Tregs), a subset of CD4-positive T cells characterized by expression of the transcription factor forkhead box P3 (FOXP3), maintain peripheral immune tolerance and limit excessive inflammation. In tumors, however, their suppressive activity can restrain immune responses against malignant cells [2,3]. Understanding their contribution to cancer therefore requires consideration of both their normal protective functions and the local conditions that sustain their activity within tumors.

The tumor stroma provides structural, vascular and metabolic support through several interacting cell populations. Cancer-associated fibroblasts (CAFs) are heterogeneous mesenchymal cells, often derived from resident fibroblasts, that remodel the extracellular matrix and produce signals affecting immune-cell localization and function [4,5]. Blood endothelial cells line blood vessels and regulate leukocyte entry into tissues, whereas lymphatic endothelial cells line lymphatic vessels and regulate tissue drainage and immune-cell trafficking [6,7]. Adipocytes are lipid-storing cells in adipose tissue; excess adiposity connects altered metabolic states and chronic inflammation with cancer development [8]. Mesenchymal stromal cells (MSCs) are heterogeneous mesenchymal populations found in tissues such as bone marrow and adipose tissue that can modify immune responses through soluble mediators and extracellular vesicles [9,10].

These interactions are clinically relevant because effective antitumor immunity requires immune cells to reach malignant cells and retain their activity after entering the tumor. Fibroblast-derived matrix and chemokines can restrict effector T-cell access, while endothelial programs regulate adhesion and passage across vessel walls [5,7]. Stromal signals can also support Treg localization and suppressive function, and Tregs can influence stromal behavior through reciprocal signaling [2,6]. Differences in CAF phenotype and spatial organization further shape the local immune environment [11,12]. Studying these relationships may help explain variation in treatment response and resistance and identify opportunities to combine immunotherapy with interventions directed at specific stromal populations or signals.

This narrative review brings together Treg interactions with CAFs, blood and lymphatic endothelial cells, adipocytes and MSCs through four themes: spatial positioning, functional programming, metabolic conditioning and reciprocal stromal remodeling. An unresolved question is how findings from distinct stromal compartments can be integrated to identify the interactions that sustain local immune suppression and offer tractable therapeutic targets. Comparing these processes across stromal compartments helps

connect shared mechanisms and cell-specific functions with therapeutic strategies and biomarker development. Figure *1* summarizes the overall framework, and Table *1* presents representative interactions and the experimental models supporting them.

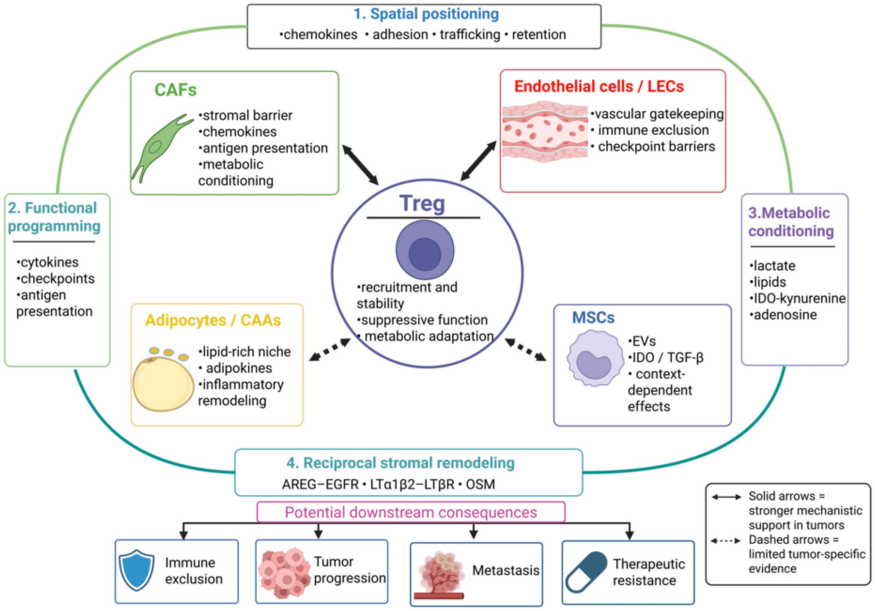


FIGURE 1: Overview of stromal-Treg interactions in the tumor microenvironment

Interactions between Tregs and CAFs, endothelial cells, adipocytes, and MSCs are grouped by spatial positioning, functional programming, metabolic conditioning, and reciprocal remodeling [2,5,6,8,9]. Solid arrows indicate stronger tumor-mechanistic support; dashed arrows indicate limited tumor-specific evidence. The named pathways and their primary studies are cited in the corresponding sections; OSM is drawn from noncancer adipose-tissue research. Downstream outcomes are schematic.

Image Credit: Yang Pan, created using BioRender (Science Suite Inc., Toronto, Ontario, Canada).

Abbreviations: AREG, amphiregulin; CAAs, cancer-associated adipocytes; CAFs, cancer-associated fibroblasts; EGFR, epidermal growth factor receptor; EVs, extracellular vesicles; IDO, indoleamine 2,3-dioxygenase; LECs, lymphatic endothelial cells; LTα1β2, lymphotoxin-α1β2; LTβR, lymphotoxin-β receptor; MSCs, mesenchymal stromal cells; OSM, oncostatin M; TGF-β, transforming growth factor-β; Tregs, regulatory T cells.

Cellular source and interaction	Disease and experimental model	Intervention	Measured endpoint and principal finding	Evidence category	Ref.
FAP-positive CAF-derived CXCL12 and T-cell exclusion	Genetically engineered mouse pancreatic cancer	FAP-positive stromal-cell depletion or CXCR4 inhibition with AMD3100, with or without PD-L1 blockade	Increased T-cell accumulation among cancer cells and improved tumor control. The demonstrated effect concerns general T-cell exclusion rather than selective Treg recruitment.	A for stromal control of T-cell exclusion	[13]
Tumor CXCL12-CXCR4 signaling and immune-cell access	Human metastatic pancreatic and microsatellite-stable colorectal cancers; paired tumor biopsies	Seven-day continuous plerixafor infusion	Increased immune-response transcriptional activity in paired biopsies. The intervention did not isolate a CAF-specific source or a selective Treg effect.	B for a CAF-Treg mechanism	[14]
CAF-derived IL-1β → CCL22 expression in oral cancer cells	Human CAF/cancer-cell cultures and oral cancer specimens	CAF IL-1β knockdown, CAF-conditioned medium and NF-κB inhibition	CAF-derived IL-1β increased cancer-cell CCL22 expression; conditioned medium from CAF-treated cancer cells promoted Treg migration in vitro.	B for the complete CAF-Treg relay	[15]
Cancer-cell CCL22 and	Syngeneic AT84 oral		Reduced tumor Foxp3 mRNA and tumor		

tumor-associated Foxp3 expression	tumors in immunocompetent C3H/HeN mice	Cancer-cell Ccl22 knockdown	growth. Treg recruitment was inferred from these findings rather than directly tracked.	B for Treg recruitment	[15]
Mesothelial-derived antigen-presenting CAFs → CD4-positive T cells	Mouse pancreatic cancer, lineage-tracing studies and antigen-specific co-cultures	Mesothelin-targeting antibody and antigen-presentation experiments	Antigen-specific conversion of naive CD4-positive cells into Tregs; mesothelin targeting reduced the mesothelial-to-apCAF transition and associated Treg formation.	A	[16]
α-SMA-positive CAF antigen processing and contact with Tregs	B16.F10 melanoma and antigen-specific CAF-Treg co-cultures	Conditional Atg5 deletion in α-SMA-positive CAFs and antigen-dependent contact assays	CAF-Treg synapse formation, Treg activation and proliferation; Atg5 deletion reduced intratumoral Tregs and tumor development.	A	[17]
IL1RL1-positive Treg-derived AREG → CAF EGFR	Mouse solid-tumor models and CAF/Treg experiments	AREG/EGFR pathway blockade and manipulation of IL1RL1 signaling	Changes in CAF profibrotic and immunosuppressive programs and tumor growth. Supports the specified Treg-to-CAF signaling direction.	A	[18]
Tumor endothelial addressins → circulating CD4-positive CD25-positive Tregs	Human pancreatic carcinoma; autologous endothelial adhesion assays and NOD/SCID xenotransplantation	Addressin-blocking antibodies	Reduced adhesion and transmigration of CD4-positive CD25-positive cells across tumor-derived endothelium. Treg identification followed the phenotyping used in the original study.	A	[19]
Endothelial FasL and differential lymphocyte survival	Human solid-tumor specimens and mouse tumor models	Genetic or pharmacologic suppression of FasL	Reduced effector CD8-positive T-cell apoptosis and increased tumor infiltration; c-FLIP-high Tregs were relatively spared by endothelial FasL.	A	[20]
Endothelial DGKG → TGF-β1-associated Treg differentiation	Human hepatocellular carcinoma specimens, endothelial-cell experiments and mouse HCC models	Endothelial DGKG suppression and combination testing with PD-1/VEGFR-2 blockade	Changes in endothelial TGF-β1 secretion, Treg differentiation, angiogenesis and tumor control.	A	[21]
Treg regulation of endothelial CXCL10	APCmin/+ intestinal tumors with inducible Treg depletion	Treg depletion and adoptive T-cell transfer	Increased endothelial CXCL10 production and T-cell migration into tumors after Treg depletion.	A	[22]
Treg regulation of endothelial nSMase2	APCmin/+ intestinal tumors and human endothelial-cell/Treg co-cultures	Treg depletion, Treg co-culture and nSMase2 inhibition	Tregs reduced endothelial nSMase2-associated programs; nSMase2 inhibition reduced adhesion/chemokine expression and T-cell entry.	A	[23]
Treg LTα1β2 → LTβR on LECs and tumor cells	B16F10 melanoma, lymphatic endothelial cultures and tumor-cell migration assays	Wild-type versus LTα-deficient Treg transfer, LTβR manipulation and pathway blockade	Changes in lymphatic endothelial junctions and remodeling, tumor-cell migration, Treg accumulation, tumor growth and metastasis. Recipient compartments were investigated separately.	A	[24]
Adipocyte-derived PGE2 → adipose-tissue Tregs	Noncancer adipose tissue in intermittent-fasting and obesity models	Adipocyte-specific COX-2 deletion and PGE2 rescue	Changes in adipose Treg proliferation and abundance, inflammation and insulin sensitivity.	C	[25]
Adipose-derived stromal-cell exosomes → CD4-positive T cells	Human cell cultures and MCF-7 breast cancer xenografts	Exposure to adipose-derived stromal-cell exosomes	Increased Treg differentiation in CD4-positive T-cell cultures; tumor growth and immune-marker changes were also reported in xenografts. The source cells were stromal cells rather than mature adipocytes.	B for the stromal-cell-Treg mechanism	[26]
MSC-derived TGF-β1 → Tregs	Human MSC, PBMC and breast cancer-cell co-cultures	MSC TGF-β1 knockdown and Treg depletion	Reduced MSC-associated Treg induction after TGF-β1 knockdown; Treg depletion partially restored immune-cell proliferation and effector activity.	B with functional support in vitro	[27]

MSC-derived PGD2 → ILC2 → IL-5-responsive Tregs	AML-associated MSC/HSPC cultures and leukemia xenotransplantation	COX-2 knockdown, CRTH2 or IL-5 blockade and Treg co-transfer	ILC2 and Treg expansion, malignant HSPC proliferation and leukemia development.	A	[28]
Umbilical cord-derived MSCs and Tregs during inflammatory carcinogenesis	AOM/DSS-induced colitis-associated colorectal cancer in mice and T-cell co-cultures	Intravenous MSC administration and MSC-conditioned-medium experiments	Increased mesenteric lymph-node Tregs, TGF-β/Smad2-associated Treg induction in vitro, reduced inflammation and fewer tumors. The contribution of Tregs to tumor protection was not isolated in vivo.	B for Treg-mediated tumor protection	[29]
Bone marrow-derived MSCs and tumor-associated Treg recruitment	Carcinogen-induced colorectal cancer in immunocompetent rats	MSC administration during cancer development, with additional radiotherapy experiments	Reduced tumor burden accompanied by increased tumor Foxp3, Il10 and Il2 mRNA expression. These transcriptional changes did not directly quantify Treg recruitment or establish Treg-dependent tumor protection.	B for the MSC-Treg mechanism	[30]

TABLE 1: Representative evidence for stromal Treg interactions and related immune regulation

Evidence categories apply to individual mechanistic claims: A, direct tumor-mechanistic evidence; B, tumor-associated or indirect evidence; C, noncancer mechanistic evidence; D, hypothesis. These categories describe the experimental setting and directness of support, rather than formal certainty or risk-of-bias ratings. Where specified, the category refers to the stated Treg-related claim rather than every finding in the cited study. Detailed definitions and decision rules are provided in Appendix B.

Abbreviations: α-SMA, α-smooth muscle actin; AML, acute myeloid leukemia; AOM, azoxymethane; apCAF, antigen-presenting cancer-associated fibroblast; AREG, amphiregulin; CAF, cancer-associated fibroblast; c-FLIP, cellular FLICE-inhibitory protein; COX-2, cyclooxygenase-2; CRTH2, chemoattractant receptor-homologous molecule expressed on Th2 cells; DGKG, diacylglycerol kinase gamma; DSS, dextran sulfate sodium; EGFR, epidermal growth factor receptor; FAP, fibroblast activation protein; FasL, Fas ligand; HCC, hepatocellular carcinoma; HSPC, hematopoietic stem and progenitor cell; ILC2, group 2 innate lymphoid cell; IL1RL1, interleukin-1 receptor-like 1; LEC, lymphatic endothelial cell; LTα1β2, lymphotoxin-α1β2; LTβR, lymphotoxin-β receptor; MSC, mesenchymal stromal cell; NF-κB, nuclear factor kappa B; nSMase2, neutral sphingomyelinase 2; PBMC, peripheral blood mononuclear cell; PGD2, prostaglandin D2; PGE2, prostaglandin E2; TGF-β, transforming growth factor-β; Treg, regulatory T cell.

Review

Literature selection and evidence appraisal

This narrative review was supplemented by an AI-assisted targeted PubMed search on November 6, 2026, covering publications from January 2023 onward. Searches combined Treg and cancer terms with terms for fibroblasts, endothelial cells, adipocytes or MSCs. Literature selection prioritized mechanistic relevance and Treg-related endpoints, with pivotal older studies retained. Evidence was grouped by experimental setting and directness of support for individual claims. Appraisal considered cell identity, perturbation specificity, functional endpoints and model context. Mechanistic findings were synthesized qualitatively. Clinical results were summarized by study and design, separating pharmacodynamic changes, single-arm activity, and randomized comparative effects. Published estimates and confidence intervals were retained where used; supplementary intervals or risk differences derived from event counts are identified, with their calculation methods, in the corresponding table notes. No independent duplicate screening, formal study-level risk-of-bias assessment, meta-analysis or meta-regression was performed. Detailed search strategies, selection procedures and evidence-classification rules are provided in Appendices A and B. A reporting self-check based on the six domains of the Scale for the Assessment of Narrative Review Articles (SANRA) is provided in Appendix C.

CAF and Treg circuits

Chemokine-Dependent Localization

CAF-derived chemokines influence where lymphocytes accumulate within tumors. In pancreatic cancer models, fibroblast activation protein (FAP)-positive CAFs are a major source of CXCL12 surrounding malignant cells. Blocking its receptor, CXCR4, increases T-cell access to cancer cells and improves responses to PD-L1 blockade [13]. Paired biopsies from patients with pancreatic or colorectal cancer also showed immune activation after short-term plerixafor treatment [14]. These findings concern the positioning of several lymphocyte populations; CXCL12-CXCR4 signaling is not selective for Tregs.

A more specific recruitment mechanism has been described in oral cancer. CAF-derived IL-1β increased CCL22 expression in cancer cells through NF-κB signaling. Silencing IL-1β in CAFs or inhibiting NF-κB reduced this response, while conditioned-medium experiments supported increased Treg migration [15]. In a syngeneic oral cancer model, knocking down Ccl22 in tumor cells reduced tumor growth and intratumoral Foxp3 expression. The study therefore connects a CAF-derived inflammatory signal to cancer-cell chemokine production, with migration assays and an in vivo Treg-associated endpoint supporting different steps of the proposed recruitment mechanism [15].

Cytokine Signaling and Antigen Presentation

CAF cytokines regulate both lymphocyte function and the surrounding stromal environment. TGF-β supports induced Treg differentiation [3], while fibroblast-associated TGF-β activity also contributes to immune exclusion. In metastatic urothelial cancer, a fibroblast TGF-β signature was associated with restricted CD8-positive T-cell infiltration and reduced response to PD-L1 blockade. Combined TGF-β and PD-L1 inhibition improved infiltration and tumor control in a mouse model with an immune-excluded phenotype [31]. This broader stromal effect complements, but is distinct from, direct regulation of Tregs.

In hepatocellular carcinoma, CAF-derived IL-6 acts through an intermediate immune population. IL-6 activates STAT3 in dendritic cells, increasing indoleamine 2,3-dioxygenase expression and generating regulatory dendritic cells that suppress conventional T-cell proliferation and support Treg expansion. Blocking IL-6, STAT3 or IDO activity reduced these effects in the experimental systems examined [32]. The relevant interaction is therefore a CAF-dendritic cell-Treg sequence.

IL-33 findings differ by experimental setting. Human laryngeal cancer samples showed an association between IL-33-positive CAFs and ST2-positive Tregs with an activated phenotype [33]. Functional experiments in murine colon cancer and melanoma models separately tested Treg-intrinsic IL1RL1/ST2 signaling and its contribution to responses to IL-33 and PD-1 blockade [18]. The human observations identify a stromal association, whereas the mouse experiments establish a functional role for signaling within Tregs.

Antigen presentation adds another layer of CAF heterogeneity. In pancreatic cancer, mesothelial-derived antigen-presenting CAFs (apCAFs) express MHC class II and promote antigen-specific Treg differentiation or expansion [16]. In non-small cell lung cancer (NSCLC), a different apCAF program was associated with poor pathological response to neoadjuvant chemoimmunotherapy. IFN-γ stimulated this state through JAK1/2-STAT1 signaling, while CAF-expressed PD-L2 supported FOXP1-positive Treg accumulation through RGMB. Functional experiments targeting this interaction reduced Treg expansion and supported combination with PD-1 blockade [34]. CAF origin, inflammatory exposure and accompanying checkpoint signals therefore help determine the consequences of antigen presentation.

Direct cellular contact has also been demonstrated. In B16 melanoma models, α-smooth muscle actin-positive CAFs processed antigens and formed antigen-dependent immunological synapses with Foxp3-positive Tregs. Conditional disruption of Atg5 in these fibroblasts altered CAF properties, reduced Treg accumulation and restrained tumor growth [17]. These experiments link fibroblast antigen processing and autophagy to local Treg responses.

CAF states can change during tumor development. In breast cancer, DPP4- and YAP-dependent transitions generated matrix-producing CAFs associated with suppressive immune neighborhoods, and functional assays identified effects on regulatory lymphocytes [35]. Such plasticity helps explain why a single CAF marker or antigen-presentation signature may capture different functions across tumors and treatment settings.

Metabolic Support and Reciprocal Remodeling

Lactate affects Tregs through several mechanisms. Tumor-infiltrating Tregs use MCT1-dependent lactate uptake to support proliferation and suppressive activity [36]. Lactate can also increase PD-1 expression through NFAT1 signaling and promote CTLA-4 expression through altered RNA splicing [37,38]. These studies identify responses within Tregs. The lactate available to them belongs to a shared tumor metabolic environment that includes malignant and stromal cells [39].

CAF metabolism can influence Tregs through chemokine production as well. In malignant pleural effusion, increased fibroblast glycolysis was linked to histone H3K18 lactylation at the CXCL16 and FOXO3 promoters and increased CXCL16 expression. This chemokine attracted CXCR6-expressing, TNFR2-positive Tregs. LDHA-deficient NIH/3T3 fibroblasts showed reduced Treg-attracting activity, which was restored by CXCL16. In mouse pleural tumor experiments, fibroblast LDHA loss reduced effusion burden and the proportion of TNFR2-positive Tregs, with CXCL16 supplementation reversing these effects [40]. This mechanism connects fibroblast metabolism to chemokine-dependent Treg positioning.

Tryptophan availability provides a further route of metabolic regulation. Kynurenine-aryl hydrocarbon receptor (AHR) signaling promotes regulatory differentiation in experimental T-cell systems [41]. Tryptophan depletion can increase AHR expression and enhance kynurenine uptake through GCN2-dependent LAT1 regulation, potentiating Treg induction [42]. These findings explain how the metabolic environment can favor regulatory responses; assigning this activity to CAFs requires identification of the relevant cellular source.

Signaling also proceeds from Tregs to fibroblasts. In murine tumor models, IL1RL1-positive Tregs produced amphiregulin, which acted on EGFR-expressing CAFs and promoted fibroblast states associated with

immune suppression [18]. This supplies a defined direction for reciprocal remodeling. TGF-β has additional roles in fibroblast activation and Treg differentiation, although its production by several cell populations makes individual cellular contributions more difficult to separate [2,3,43].

The disease background can determine whether an interaction becomes a useful therapeutic target. In steatotic liver disease-related hepatocellular carcinoma, spatial analyses identified close Treg-fibroblast neighborhoods associated with immunotherapy resistance. Blocking TNFRSF14 together with PD-1 improved tumor control, reduced intratumoral Treg proportions and increased active CD8-positive T cells in high-fat-diet mouse models. The same enhancement was not observed in mice without prior high-fat feeding [44]. These results support evaluating stromal-Treg interactions within the underlying metabolic and tissue context.

Treatment selection should consequently reflect the dominant CAF state and its immune partners. Broad CAF depletion may remove protective as well as suppressive functions [4,5]. NNMT inhibition illustrates a more selective approach: studies centered on ovarian cancer linked CAF metabolic reprogramming to reduced myeloid recruitment and improved antitumor immunity [45]. Its principal reported immune effects involved myeloid cells and CD8-positive T cells, emphasizing the need to distinguish general stromal reprogramming from interventions that directly alter Treg-dependent suppression. Figure *2* summarizes the CAF-associated mechanisms discussed here.

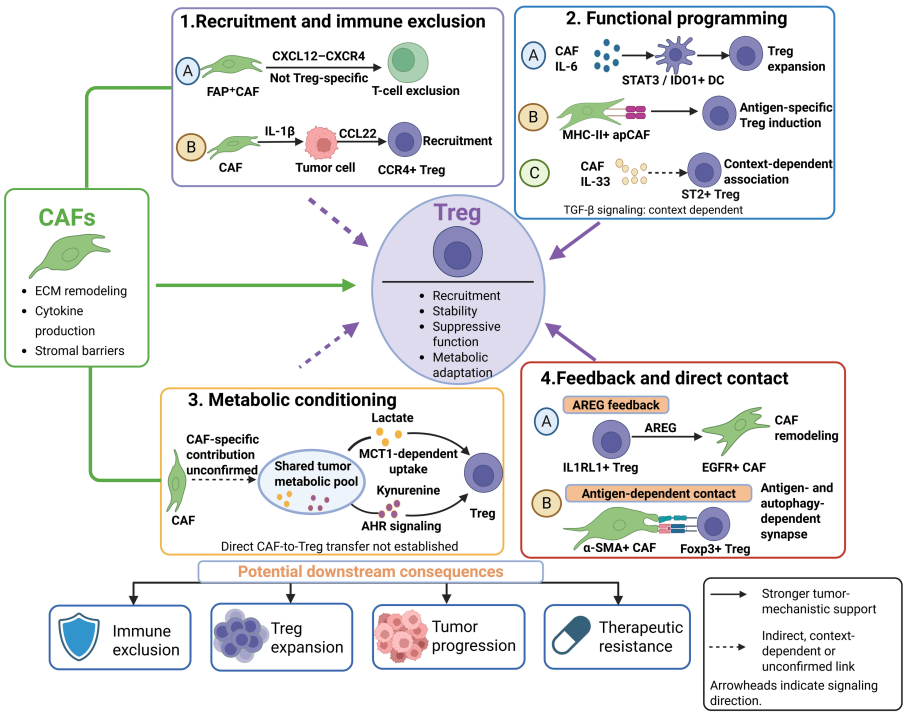


FIGURE 2: Cancer-associated fibroblast-Treg interactions

The panels summarize CAF-related T-cell exclusion and Treg recruitment [13,15], apCAF and IL-6-DC programming [16,32], an IL-33-ST2 association [33] and TGF-β-related T-cell exclusion [31], Treg lactate and kynurenine responses without a proven CAF source [36,42], and antigen-dependent contact or AREG-EGFR feedback [17,18]. Solid black arrows indicate stronger tumor-mechanistic support; dashed arrows indicate indirect or context-dependent links. Colored connectors group the panels, and downstream outcomes are schematic.

Image Credit: Yang Pan, created using BioRender (Science Suite Inc., Toronto, Ontario, Canada).

Abbreviations: α-SMA, α-smooth muscle actin; AHR, aryl hydrocarbon receptor; apCAF, antigen-presenting CAF; AREG, amphiregulin; CAF, cancer-associated fibroblast; CCL22, C-C motif chemokine ligand 22; CCR4, C-C motif chemokine receptor 4; CXCL12, C-X-C motif chemokine ligand 12; CXCR4, C-X-C motif chemokine receptor 4; DC, dendritic cell; ECM, extracellular matrix; EGFR, epidermal growth factor receptor; FAP, fibroblast activation protein; Foxp3, forkhead box P3; IDO1, indoleamine 2,3-dioxygenase 1; IL, interleukin; IL1RL1/ST2, interleukin-1 receptor-like 1; MCT1, monocarboxylate transporter 1; MHC-II, major histocompatibility complex class II; STAT3, signal transducer and activator of transcription 3; TGF-β, transforming growth factor-β; Treg, regulatory T cell.

Endothelial and Treg circuits

Physiological Trafficking and Tissue-Specific Regulation

Blood and lymphatic endothelial cells regulate different stages of Treg trafficking. High endothelial venules support lymph-node entry through L-selectin and CCR7-dependent homing, while chemokine presentation by heparan sulfate and integrin-mediated adhesion help coordinate endothelial passage. Lymphatic vessels provide routes from peripheral tissues to draining lymph nodes [6]. These physiological processes provide a starting point for understanding how vascular beds influence Treg distribution in tumors.

Some endothelial populations also regulate Treg differentiation. In mouse liver-cell systems, liver sinusoidal endothelial cells (LSECs) induced antigen-specific Foxp3-positive Tregs through TGF-β-dependent signaling. The induced cells suppressed effector responses in vitro and experimental autoimmune encephalomyelitis in vivo [46]. Human umbilical-vein endothelial cells similarly promoted Foxp3 induction in maternal T-cell co-cultures, partly through TGF-β [47]. These studies describe hepatic and pregnancy-associated tolerance, providing defined noncancer settings for comparison with tumor endothelium.

CLEVER-1/stabilin-1 supports preferential Treg transmigration across human hepatic sinusoidal endothelium. Its expression in inflamed liver vessels and hepatocellular carcinoma-associated vasculature links this trafficking mechanism to hepatic inflammation and cancer. In primary human hepatic sinusoidal endothelial cultures under flow, CLEVER-1 blockade reduced Treg passage, with greater inhibition when ICAM-1 and vascular adhesion protein-1 were also blocked [48].

Antigen recognition can participate directly in endothelial control of Treg localization. In inflammatory mouse models, recognition of self-antigens presented by IFN-γ-stimulated endothelium promoted Treg transmigration and recruitment to target tissues through MHC class II and T-cell receptor signaling [49]. At the lymphatic interface, endothelial PD-L1 regulates activated CD4 T-cell passage through distinct binding partners: PD-1 on Tregs and CD80 on conventional effector T cells. Disrupting these interactions impairs transendothelial migration in vitro and alters T-cell egress from tumors to draining lymph nodes in vivo [50].

Tumor Endothelial Immune Barriers

Tumor endothelium can favor Treg entry through selective adhesion. In human pancreatic carcinoma, patient-derived endothelial assays and xenograft experiments showed preferential Treg adhesion and transmigration. Antibody blockade implicated endothelial addressins, including MAdCAM-1, VCAM-1, CD62-E and CD166, in this process [19]. This provides a recruitment mechanism distinct from the loss of effector-cell access.

Other vascular programs restrict lymphocyte adhesion and entry. Basic fibroblast growth factor sustains endothelial p38-MAPK activity and inhibits inflammatory NF-κB signaling, reducing ICAM-1 expression [51]. Histone modifications can further silence endothelial ICAM-1 [52]. EGFL7 suppresses endothelial activation [53], while endothelin B receptor signaling impairs T-cell adhesion and tumor homing, including in ovarian cancer-associated vascular models [54]. These mechanisms contribute to endothelial anergy and reduced responsiveness to inflammatory recruitment signals.

Endothelial filtering also operates through differential survival. VEGF-A, IL-10 and prostaglandin E2 induce endothelial Fas ligand, which promotes effector CD8 T-cell apoptosis. Tregs are relatively resistant because of higher c-FLIP expression [20]. Restricted effector entry and selective elimination can therefore increase the Treg proportion without increasing the absolute number of Tregs. This compositional change differs from selective recruitment, local expansion or differentiation.

Hepatocellular carcinoma illustrates the functional diversity of tumor endothelial states. CXCL12-positive endothelial cells inhibit differentiation of naive CD8 T cells into cytotoxic cells and recruit myeloid-derived suppressor cells [55]. A separate hypoxia-induced DGKG program recruits USP16 to stabilize ZEB2, increasing endothelial TGF-β1 secretion and promoting both angiogenesis and Treg differentiation. Targeting endothelial DGKG improved combined PD-1 and VEGFR2 blockade in mouse hepatocellular carcinoma models [21]. These endothelial programs affect different immune populations and offer different grounds for selecting combination treatments.

Checkpoint and metabolic signals add further layers of vascular immune regulation. In nasopharyngeal carcinoma models, tumor-conditioned endothelial cells upregulated PD-L1 through NF-κB-STAT3 signaling, reducing T-cell-mediated killing [56]. In B16 melanoma, CD40 agonism increased T-cell-derived IFN-γ, which induced endothelial IDO1 as a treatment-associated inhibitory feedback mechanism [57]. CD73 studies distinguished nonhematopoietic control of T-cell homing from hematopoietic effects on T-cell expansion and effector function [58]. Adenosine-mediated suppression consequently spans vascular, other stromal and immune compartments [58,59].

Fibroblast barriers and vascular filtering can restrict successive steps of lymphocyte access [5,59]. Vascular normalization may improve perfusion and entry, while checkpoint or metabolic interventions address inhibitory signals encountered within the lesion. This provides a mechanistic rationale for combining vascular and immune interventions, with treatment selection informed by the barriers operating in the relevant tumor setting [60].

The intratumoral CD8-to-Treg balance reflects the combined effects of recruitment, lymphatic egress, proliferation and survival. Absolute cell densities and subset proportions provide complementary information about this balance. Interpreting these measures alongside endothelial adhesion and directional migration helps identify changes in tissue entry or lymphatic exit, while proliferation and apoptosis measurements clarify contributions from local expansion and differential survival. Functional suppression assays further determine whether Foxp3 induction is accompanied by regulatory activity [6,59].

Reciprocal Endothelial Remodeling

Tregs can maintain vascular conditions that limit further lymphocyte recruitment. In intestinal tumors of APCmin/+ mice, Treg depletion increased endothelial CXCL10 production and CXCR3-dependent T-cell entry [22]. Subsequent work identified endothelial neutral sphingomyelinase 2 as a mediator of this effect. Treg co-culture reduced endothelial nSMase2, while pharmacological inhibition lowered VCAM-1, CX3CL1 and CXCL10 and limited the increased tumor entry observed after Treg depletion [23]. These findings connect Treg activity to endothelial chemokine production and adhesion.

Lymphotoxin signaling extends this feedback to lymphatic vessels and tumor cells. Treg-expressed LTα1β2 stimulates LTβR nonclassical NF-κB signaling in both compartments. In B16F10 melanoma experiments, this interaction promoted tumor growth and lymphatic migration, while pathway-selective blockade reduced lymphatic metastasis and altered intratumoral immune composition [24]. The mechanism involves communication among Tregs, lymphatic endothelium and malignant cells, with contributions from both recipient compartments.

Tumor cells can also initiate a vascular feedback sequence. Hypoxia-induced tumor-cell CCL28 recruits Tregs and promotes angiogenesis [61]. Here, the initiating chemokine comes from malignant cells, while the vascular response develops downstream of Treg recruitment. Figure *3* illustrates selected endothelial-Treg interactions together with their physiological trafficking context.

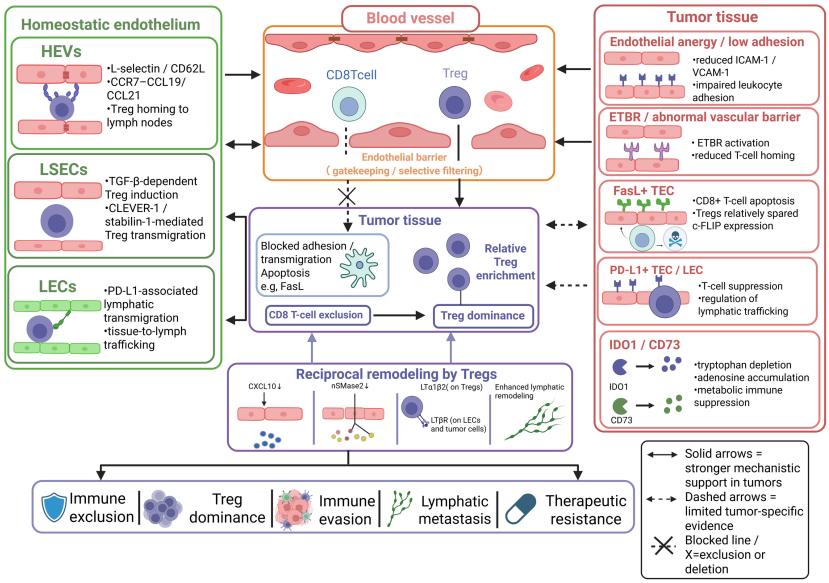


FIGURE 3: Endothelial regulation of lymphocyte trafficking and reciprocal remodeling by Tregs

The left panel places HEV-associated homing, LSEC-mediated Treg induction or transmigration, and LEC passage in physiological or noncancer contexts [6,46,48,50]; tumor endothelial selection involves adhesion and ETBR [19,52,54], FasL-mediated effector-cell loss with relative Treg sparing [20], and PD-L1, IDO1 or CD73 activity [56-58], while Treg feedback involves CXCL10, nSMase2 and LTα1β2-LTβR [22-24]. For tumor-associated links, solid arrows denote stronger mechanistic support and dashed arrows indicate limited tumor-specific evidence; the crossed CD8 route denotes exclusion or loss, and outcomes are schematic.

Image Credit: Yang Pan, created using BioRender (Science Suite Inc., Toronto, Ontario, Canada).

Abbreviations: CCL19/CCL21, C-C motif chemokine ligands 19 and 21; CCR7, C-C motif chemokine receptor 7; CD62L, L-selectin; CD73, ecto-5′-nucleotidase; c-FLIP, cellular FLICE-inhibitory protein; CLEVER-1, common lymphatic endothelial and vascular endothelial receptor-1 (stabilin-1); CXCL10, C-X-C motif chemokine ligand 10; ETBR, endothelin B receptor; FasL, Fas ligand; HEVs, high endothelial venules; ICAM-1, intercellular adhesion molecule 1; IDO1, indoleamine 2,3-dioxygenase 1; LECs, lymphatic endothelial cells; LSECs, liver sinusoidal endothelial cells; LTα1β2, lymphotoxin-α1β2; LTβR, lymphotoxin-β receptor; nSMase2, neutral sphingomyelinase 2; PD-L1, programmed death-ligand 1; TEC, tumor endothelial cell; TGF-β, transforming growth factor-β; Tregs, regulatory T cells; VCAM-1, vascular cell adhesion molecule 1.

Adipocyte and Treg interactions

Mechanisms Established in Adipose Tissue

Adipose tissue connects systemic metabolic status with inflammatory, endocrine and nutrient conditions relevant to cancer [8]. Within individual depots, mature adipocytes, stromal precursors and resident immune cells contribute differently to tissue function. Visceral adipose Tregs have a specialized PPAR-γ-dependent program that supports their accumulation and phenotype [62,63]. Their interactions with neighboring cells provide a mechanistic foundation for understanding immune regulation in lipid-rich tissues.

Nutritional and endocrine signals influence this population through several routes. In intermittent-fasting mouse models, adipocyte COX-2-dependent PGE2 promoted Treg proliferation through CaMKII signaling and contributed to improved insulin sensitivity [25]. Human Treg experiments also identified an autocrine leptin pathway that restrained proliferation, with leptin neutralization permitting expansion of suppressive Tregs [64]. Cold exposure and β3-adrenergic stimulation linked environmental inputs to Treg induction and adipose function through a T-cell STAT6-PTEN pathway [65].

Tregs also regulate adipose metabolism through their cytokine output. In diet-induced obesity models, deletion of the p38 activators MKK3/6 in CD4 and CD8 T cells increased Treg accumulation and enhanced thermogenesis. Complementary human and mouse Treg experiments identified p38-dependent control of IL-35 production, while IL-35 promoted an adipocyte thermogenic program involving ATF2, UCP1 and FGF21 [66]. These results connect a broader T-cell signaling intervention with a defined Treg cytokine mechanism in metabolic disease.

Other Treg-derived signals act on adipose precursors and mature-tissue responses. Oncostatin M restrained stromal adipocyte-precursor differentiation, and deletion of OSM in Tregs or its receptor in stromal cells impaired insulin sensitivity [67]. In high-fat-diet-fed male mice, Treg-derived IL-10 suppressed white-adipose beiging; Treg-specific loss of IL-10 or its regulator Blimp-1 improved insulin sensitivity and reduced obesity [68]. The metabolic consequences of Treg activity therefore vary with the recipient population, cytokine program and nutritional setting.

Evidence in Tumors

Tumor-bearing adipose tissue provides direct evidence of Treg recruitment and local adaptation. In mouse omental tumor models, parabiosis, cell tracking and T-cell receptor profiling showed that Treg accumulation was driven predominantly by recruitment from the circulation. Newly recruited cells acquired transcriptional, homing and metabolic features associated with adipose-resident Tregs, and the preexisting Treg repertoire was sufficient to suppress antitumor immunity and support tumor growth [69]. These findings place Treg adaptation within the changing immune environment of tumor-associated fat.

Lipid metabolism supports Treg function through programs that differ between tissue environments. PPAR-γ contributes to Treg specialization in noncancer visceral adipose tissue [62,63], while CD36 supports mitochondrial fitness in tumor-infiltrating Tregs through PPAR-β signaling. The functional importance of this adaptation is evident from Treg-specific Cd36 deletion, which impaired intratumoral Treg survival and suppressive activity and improved tumor control [70].

Adipocytes can simultaneously support malignant-cell metabolism. In prostate cancer experiments, tumor-derived extracellular vesicles induced lipolysis in differentiated 3T3-L1 adipocytes through reduced G0S2 expression, increased ATGL expression and activation of cAMP-PKA-HSL signaling. Fatty acids released by the treated adipocytes then increased prostate cancer-cell proliferation, migration and invasion through Akt-associated responses [71]. This interaction links tumor-derived vesicles to adipocyte remodeling and subsequent lipid-dependent tumor behavior.

A different vesicle-mediated mechanism has been described in colorectal signet ring cell carcinoma. Cancer-associated adipocytes isolated from omental metastatic sites increased fatty-acid availability and promoted patient-derived tumor-organoid growth. Adipocyte-derived exosomes induced FABP4 expression in the malignant organoids, supporting fatty-acid oxidation, stemness and peritoneal metastatic capacity. Silencing FABP4 in the organoids attenuated these effects [72]. The induced FABP4 program was therefore located in the malignant recipient cells.

Adipose-derived stromal cells provide another route of immune regulation. Exosomes isolated from human adipose-derived stromal cells were taken up by CD4 T cells and promoted Treg differentiation in co-culture. The same preparations influenced macrophage polarization and enhanced MCF-7 tumor growth in nude mice [26]. These findings identify stromal-cell vesicles as an immunoregulatory component of adipose-tumor interactions, with Treg differentiation and tumor growth assessed in their respective experimental systems.

Breast cancer atlases further resolve the cellular organization of tumor-associated fat. Single-nucleus profiling identified LDLR-high adipocyte and precursor populations enriched in estrogen receptor-positive disease, together with an LGR4/TGFBR1-expressing precursor population prominent in triple-negative breast cancer. Cell-communication analysis highlighted putative interactions with macrophages, while immunofluorescence linked selected markers to recurrence [73]. A complementary study in patients with high BMI identified changes in mature FKBP5-positive adipocytes, macrophages and APOD-positive γδ T cells, together with inferred changes in EGF, CXCL and CCL communication networks [74]. These studies place adipocyte heterogeneity within multicellular immune and stromal neighborhoods.

Adipose remodeling links malignant-cell nutrient use with Treg recruitment and metabolic adaptation through mechanisms operating in different cellular compartments. FABP4 targeting can alter malignant-cell metabolism [72], whereas CD36 targeting can impair the survival and suppressive function of tumor-infiltrating Tregs [70]. The PPAR-γ-dependent specialization of Tregs in noncancer visceral adipose tissue further illustrates how local metabolic programs shape immune regulation [62,63]. These distinctions make the cellular site of action central to interpreting the therapeutic effects of interventions involving adipose tissue and Tregs.

MSC and Treg interactions

Evidence Outside Cancer

MSC immunoregulation varies with tissue source, donor condition, culture format and inflammatory exposure [9,10]. Extracellular-vesicle studies illustrate several of these differences. Vesicles from three-dimensional cultures of human umbilical-cord MSCs enhanced Treg responses in experimental vitiligo, with miR-132-3p contributing to their immunomodulatory activity [75]. Human gingival MSC vesicles regulated

Treg/Th17 differentiation through miR-148a-3p and IKKβ/NF-κB signaling in arthritis [76]. Donor disease state also affected vesicle function: exosomes from bone-marrow MSCs of patients with lupus had impaired Treg-promoting activity, which was restored by miR-20a-5p enrichment [77].

MSCs influence Tregs through myeloid intermediates as well as direct contact. Under GM-CSF stimulation, human bone-marrow MSCs induced suppressive myeloid populations from mouse bone marrow. A CSF-1R-high subset inhibited CD4 T-cell proliferation and promoted Treg expansion in culture and experimental autoimmune uveoretinitis [78]. In a corneal transplantation model, mouse bone-marrow MSCs enhanced Treg FoxP3 expression and suppressive function through CD80-dependent interactions. CD80 blockade in co-culture and MSC CD80 silencing in vivo attenuated these effects [79]. Tissue access provides another source of variation: E-cadherin-directed chimeric antigen receptors enhanced the localization and T-cell-suppressive activity of human adipose-derived MSCs in graft-versus-host disease models [80].

Tumor-Specific and Context-Dependent Effects

Breast cancer cocultures provide functional evidence that MSCs can protect malignant cells partly through Tregs. Human MSCs increased Treg frequency and suppressed cytotoxic lymphocyte activity in co-cultures containing peripheral blood mononuclear cells and breast cancer cells. MSC TGFB1 knockdown limited the Treg increase, while Treg depletion partially restored immune-cell proliferation and effector function [27]. Human adipose-derived stromal-cell exosomes also promoted Treg differentiation in vitro and increased breast tumor growth in mice [26].

MSC origin can alter the myeloid contribution to T-cell regulation. A recent cervical cancer study compared MSCs isolated from tumor tissue with those from normal cervix. Compared with the normal-tissue condition, tumor-cell/tumor-derived MSC cocultures generated macrophages with higher IDO and IL-10 expression and stronger inhibition of T-cell proliferation. These macrophages also generated a higher proportion of $CD4^+CD25^+FOXP3^+$ cells in subsequent CD4 T-cell cocultures [81]. The comparison connects the tissue state of MSCs to immune regulation through a macrophage intermediary.

In acute myeloid leukemia, patient-derived MSCs supported a defined PGD2-dependent interaction with innate lymphoid cells and Tregs. MSC-derived PGD2 activated CRTH2 on type 2 innate lymphoid cells, increasing IL-5 production and expanding IL-5 receptor-positive Tregs. These Tregs promoted normal and malignant hematopoietic progenitor proliferation through IL-10 signaling, and their co-transfer accelerated leukemia development in xenografted mice [28].

IDO- and stanniocalcin-1-associated programs also affect antitumor effector cells, with different accompanying Treg responses. In melanoma and lymphoma models, iNOS-deficient mouse MSCs engineered to express human IDO promoted tumor growth and reduced intratumoral CD8 T cells and B cells without significantly changing Treg frequency [82]. In a separate lymphoma study, MSC-derived stanniocalcin-1 (STC1) impaired CAR-T activity. STC1 knockdown improved CAR-T killing, altered CD4/CD8 composition and reduced phenotypically defined Treg frequencies in co-culture and FOXP3-positive tumor infiltrates [83]. The study linked STC1 to treatment resistance and Treg-associated changes, although Treg dependence was not directly tested.

The consequences of MSC-induced immune regulation are particularly sensitive to the inflammatory setting and treatment schedule in colorectal cancer. Intravenous umbilical-cord MSC administration increased mesenteric lymph node Tregs and reduced inflammation and tumor formation in an AOM/DSS model [29]. Bone-marrow MSCs also attenuated carcinogenesis in an MNNG-induced rat model, accompanied by increased tumor Foxp3 and Il10 expression [30]. A subsequent AOM/DSS study directly compared early and late intraperitoneal administration of bone-marrow MSCs. Early treatment increased Tregs through TGF-β-associated regulation and suppressed tumor development, whereas late treatment promoted an IL-4-associated Th2 shift and tumor progression [84]. This timing comparison separates protection associated with control of early inflammation from the tumor-promoting effects of later immune polarization.

MSC-mediated immune regulation can restrain inflammation-associated tumor initiation or support established tumors, depending on tissue origin, disease stage, and treatment timing. These distinctions make the biological state of the MSC population central to interpreting its therapeutic effects.

Integrated Evidence Across Stromal Compartments

Stromal regulation of Tregs links access to the tumor with the signals that sustain immune suppression after entry. Chemokine gradients, extracellular matrix organization and endothelial barriers determine where lymphocytes accumulate, while antigen presentation, cytokines and local nutrient availability influence their subsequent activity. Treg-derived signals can then modify the stromal environment in which these responses develop [16-18,22-24,36-38]. These processes can reinforce one another: increased immune-cell entry may coexist with persistent local suppression, whereas changes in stromal signaling may have limited effects when effector cells remain excluded. This functional coupling provides a rationale for combinations that address both tissue access and immune activity within the tumor.

The contribution of each compartment depends on its cellular composition and anatomical setting. Fibroblast states associated with matrix deposition or Treg support differ from CCL19-positive fibroblastic reticular cell-like populations associated with lymphoid organization and favorable immunotherapy outcomes [11,35,85]. Blood and lymphatic endothelial cells regulate distinct routes of entry and exit, and their effects vary across vascular beds [6,7]. Adipose-associated mechanisms also involve different cellular participants, including mature adipocytes, stromal precursors and lipid-adapted Tregs. MSC effects are similarly shaped by tissue origin and the inflammatory conditions in which they act [9]. Stromal abundance alone therefore provides an incomplete account of immune function; the relevant information lies in the cell states present, their spatial relationships and the signals exchanged between them.

This heterogeneity makes cellular and spatial context central to therapeutic selection. A useful biomarker should connect a target to the stromal population expressing it and to the immune process that treatment is intended to change. Spatial profiling can identify such relationships, while tissue collected during treatment can show whether an intervention alters immune access, local Treg activity or stromal organization [85-87]. These measurements offer a biological basis for selecting combinations and interpreting response. The therapeutic aim is to interrupt the interactions sustaining suppression in a particular tumor while preserving stromal functions that support effective immunity.

Clinical and Translational Implications

Clinical studies have examined several pathways involved in stromal regulation of Tregs, with different levels of evidence for immune modulation and treatment benefit. In metastatic pancreatic cancer, the initial COMBAT study associated motixafortide plus pembrolizumab with increased intratumoral CD8 T-cell infiltration and reduced circulating Tregs [88]. The expanded cohort evaluated this combination with nanoliposomal irinotecan, fluorouracil and folinic acid in 43 patients, including 38 evaluable for response. The objective response rate (ORR) was 21.1% (8/38; 95% CI, 9.6-37.3%), with confirmed responses in 13.2% (5/38; 95% CI, 4.4-28.1%) [89]. These findings support further clinical evaluation of the combination, although its single-arm design does not establish the incremental benefit of CXCR4 inhibition.

CCR4-directed treatment provides a more direct link between Treg depletion and tissue pharmacodynamics. Mogamulizumab plus nivolumab produced responses in 12 of 114 patients with advanced solid tumors, an ORR of 10.5% (95% CI, 5.6-17.7%) [90]. A separate neoadjuvant study enrolled 16 patients and demonstrated depletion of intratumoral CCR4-positive Foxp3-positive cells in evaluable paired specimens. Clinical and pathological responses were assessed separately: three patients had a clinical partial response, while the 15 resected tumors included one pathological complete response and nine pathological partial responses [86]. The tissue findings establish local pharmacodynamic activity, whereas the uncontrolled response results provide preliminary evidence of antitumor activity.

Randomized trials have yielded less consistent results for broader immunoregulatory targets. In 304 patients with treatment-naïve, PD-L1-high advanced NSCLC, bintrafusp alfa did not demonstrate superiority over pembrolizumab. Hazard ratios were 1.232 (95% CI, 0.885-1.714) for progression-free survival (PFS) and 1.201 (95% CI, 0.796-1.811) for overall survival (OS). Grade ⩾3 treatment-related adverse events occurred in 64 of 151 versus 20 of 152 treated patients [91]. The higher rate of severe treatment-related toxicity underscores the need to evaluate the safety cost of combined TGF-β and PD-L1 inhibition alongside any therapeutic benefit.

Vascular-immune combinations have demonstrated comparative benefit in defined disease settings. In IMpower150, adding atezolizumab to bevacizumab, carboplatin and paclitaxel improved PFS and OS relative to bevacizumab, carboplatin and paclitaxel in the primary population without EGFR or ALK alterations. The respective hazard ratios were 0.62 (95% CI, 0.52-0.74) and 0.78 (95% CI, 0.64-0.96) [92]. This comparison evaluates the addition of atezolizumab to a bevacizumab-containing chemotherapy regimen.

In previously untreated unresectable hepatocellular carcinoma, IMbrave150 compared atezolizumab plus bevacizumab with sorafenib. At the primary analysis, the hazard ratios were 0.59 (95% CI, 0.47-0.76) for PFS and 0.58 (95% CI, 0.42-0.79) for OS [93]. These trials support the efficacy of their respective regimens. Improved vascular access and changes in local immune regulation offer plausible mechanistic explanations, but the clinical comparisons do not identify a specific Treg-dependent mechanism.

Metabolic targeting has also produced mixed results. In the randomized expansion of an oleclumab study in untreated metastatic pancreatic cancer, patients received gemcitabine plus nab-paclitaxel alone, with oleclumab, or with oleclumab and durvalumab. The primary comparison of the triple combination against chemotherapy showed an ORR difference of 3.8 percentage points (95% CI, -13.2 to 20.7; p = 0.650). PFS and OS hazard ratios were 0.72 (95% CI, 0.47-1.11) and 0.75 (95% CI, 0.50-1.13), respectively [94]. Findings in tumors with high CD73 expression were exploratory and provide a hypothesis for biomarker selection.

In ECHO-301/KEYNOTE-252, adding epacadostat to pembrolizumab did not improve outcomes in unresectable or metastatic melanoma. The PFS hazard ratio was 1.00 (95% CI, 0.83-1.21; one-sided p = 0.52), and the OS hazard ratio was 1.13 (95% CI, 0.86-1.49; one-sided p = 0.81) [95]. The result illustrates the gap

between a metabolic mechanism implicated in immune suppression and an effective therapeutic intervention at the tested dose and schedule.

Spatial studies help define the biological settings in which these interventions might be most informative. The metastatic breast cancer atlas described variation in cellular composition and spatial organization across clinicopathological contexts [96]. Associations with immunotherapy outcomes were examined more directly in studies of fibroblast-associated immune niches and NSCLC spatial signatures [85,87]. In particular, the association of fibroblastic reticular cell-like populations with favorable immune organization shows why fibroblast-rich tumors cannot be treated as a single immunosuppressive category. Such observations support biomarkers that capture stromal state and immune organization together.

Serial tissue analysis can connect baseline stromal features to treatment-associated changes. In an initial 11-patient cohort of a phase II study of motixafortide, cemiplimab, gemcitabine and nab-paclitaxel in metastatic pancreatic cancer, single-nucleus profiling of serial biopsies identified treatment-associated changes in tumor cell states and enrichment of CXCL12-positive CAFs in responders [97]. Together with the paired-tissue CCR4 study [86], these exploratory findings support integrating stromal phenotypes, Treg measurements and immune localization into early clinical trials.

Several biological features may explain why pathway-directed interventions differ in clinical activity. Targets can be shared by suppressive and effector populations, stromal states vary between tumors, and parallel signals may sustain suppression after one pathway is inhibited. In the mogamulizumab study, depletion of CCR4-expressing effector populations was proposed as one possible counterweight to Treg depletion [90]. These considerations favor testing combinations in tumors with a defined target-associated phenotype and assessing tissue pharmacodynamics alongside clinical outcomes. Tolerability remains part of that assessment: the neoadjuvant CCR4 study reported grade 3-4 treatment-related adverse events in 6 of 16 patients [86], while the bintrafusp alfa trial demonstrated greater severe treatment-related toxicity than its comparator [91]. Tables *2*-*3* distinguish pharmacodynamic observations and single-arm activity from randomized comparative treatment effects.

Study and population	Intervention	Main findings	Interpretation
COMBAT: initial cohort, n = 37; expanded chemotherapy cohort, 43 enrolled and 38 response-evaluable [88,89]	Motixafortide plus pembrolizumab; the expanded cohort also received nanoliposomal irinotecan, fluorouracil and folinic acid	Initial study: increased intratumoral CD8 T-cell infiltration and reduced circulating Tregs. Expanded cohort: ORR 8/38, 21.1% (95% CI, 9.6-37.3%); confirmed ORR 5/38, 13.2% (95% CI, 4.4-28.1%).[a]	Pharmacodynamic changes and single-arm activity; the incremental effect of CXCR4 inhibition was not estimated
Phase I/II study in advanced solid tumors, n = 114 [90]	Mogamulizumab plus nivolumab	ORR 12/114, 10.5% (95% CI, 5.6-17.7%); depletion of effector Tregs was observed	No concurrent nivolumab-only comparator
Phase I neoadjuvant study in mixed operable solid tumors, n = 16; 15 underwent resection [86]	Mogamulizumab plus nivolumab before surgery	Intratumoral CCR4-positive Foxp3-positive cells decreased in evaluable paired specimens. Clinical PR: 3/16. Pathological responses among 15 resected tumors: 1 CR and 9 PRs. Grade 3-4 TRAEs: 6/16 (37.5%).[b]	Paired tissue demonstrates local pharmacodynamic activity; clinical and pathological responses are separate endpoints

TABLE 2: Nonrandomized clinical studies of stromal and Treg directed interventions

Notes. Results refer to the cited publications. Single-arm response rates describe treatment activity and should not be interpreted as comparative treatment effects. Clinical outcomes do not identify which cellular compartment mediated the response.

[a] For the expanded COMBAT cohort, exact 95% confidence intervals were calculated for this review using the Clopper-Pearson method with the response-evaluable denominator of 38. The other confidence interval is reported as published.

[b] The neoadjuvant study additionally reported one grade 5 interstitial pneumonia event; the authors attributed the patient's death to disease progression. Pathological PR comprised tumor regression grades 1-2 and should not be relabeled as major pathological response.

Abbreviations. CCR4, C-C motif chemokine receptor 4; CI, confidence interval; CR, complete response; CXCR4, C-X-C motif chemokine receptor 4; Foxp3, forkhead box P3; ORR, objective response rate; PR, partial response; TRAE, treatment-related adverse event; Treg, regulatory T cell.

Study and analysis population	Intervention and comparator	Main findings	Interpretation
Phase III bintrafusp alfa trial; 152 patients per randomized group; safety populations 151 and 152 [91]	Bintrafusp alfa versus pembrolizumab in treatment-naïve, PD-L1-high advanced NSCLC	PFS HR 1.232 (95% CI, 0.885-1.714); OS HR 1.201 (95% CI, 0.796-1.811). Grade ≥3 TRAEs: 64/151 (42.4%) versus 20/152 (13.2%). Risk difference: 29.2 percentage points (95% CI, 19.4-38.4).[a]	Superiority was not demonstrated; severe treatment-related toxicity was greater with bintrafusp alfa
IMpower150; primary EGFR/ALK-wild-type comparison, n = 356 versus 336 [92]	Atezolizumab, bevacizumab, carboplatin and paclitaxel versus bevacizumab, carboplatin and paclitaxel	PFS HR 0.62 (95% CI, 0.52-0.74); OS HR 0.78 (95% CI, 0.64-0.96)	Benefit from adding atezolizumab to bevacizumab-chemotherapy; one comparison within a three-arm trial
IMbrave150; untreated unresectable HCC, n = 336 versus 165 [93]	Atezolizumab plus bevacizumab versus sorafenib	Primary-analysis PFS HR 0.59 (95% CI, 0.47-0.76); OS HR 0.58 (95% CI, 0.42-0.79)	Comparative benefit of the combination in this disease setting
Oleclumab randomized expansion; untreated metastatic PDAC, n = 170 [94]	A1: GnP, n = 62 A2: oleclumab plus GnP, n = 38 A3: oleclumab plus durvalumab plus GnP, n = 70	ORR: A1, 18/62 (29.0%); A2, 8/38 (21.1%); A3, 23/70 (32.9%). Primary A3-A1 ORR difference: 3.8 percentage points (95% CI, -13.2 to 20.7; p = 0.650). A3 versus A1: PFS HR 0.72 (95% CI, 0.47-1.11); OS HR 0.75 (95% CI, 0.50-1.13).	Primary efficacy endpoint was not met; CD73-high subgroup findings were exploratory
ECHO-301/KEYNOTE-252; unresectable or metastatic melanoma, n = 354 versus 352 [95]	Epacadostat plus pembrolizumab versus placebo plus pembrolizumab	PFS HR 1.00 (95% CI, 0.83-1.21; one-sided p = 0.52); OS HR 1.13 (95% CI, 0.86-1.49; one-sided p = 0.81)	Addition of epacadostat did not demonstrate improved PFS or OS

TABLE 3: Randomized clinical studies of stromal and immune regulatory interventions

Notes. Results refer to the analyses in the cited publications. Hazard ratios compare the intervention with its stated comparator. IMpower150 and IMbrave150 results are from their cited primary reports. Comparative efficacy does not establish a Treg-dependent mechanism.

[a] The bintrafusp alfa toxicity risk difference and its 95% confidence interval were calculated for this review from published event counts using the Newcombe method based on Wilson score intervals. Other confidence intervals and the oleclumab ORR difference are reported as published.

Abbreviations. ALK, anaplastic lymphoma kinase; CD73, ecto-5′-nucleotidase; CI, confidence interval; EGFR, epidermal growth factor receptor; GnP, gemcitabine plus nab-paclitaxel; HCC, hepatocellular carcinoma; HR, hazard ratio; NSCLC, non-small cell lung cancer; ORR, objective response rate; OS, overall survival; PDAC, pancreatic ductal adenocarcinoma; PD-L1, programmed death-ligand 1; PFS, progression-free survival; TRAE, treatment-related adverse event; Treg, regulatory T cell.

Limitations

This narrative review did not use independent duplicate screening or a formal risk-of-bias assessment, and literature selection may have been influenced by publication and selection biases. Mechanistic studies differed in species, tumor models, stromal cell definitions and experimental interventions, limiting direct comparison across compartments. Evidence from noncancer tissues informs biological interpretation but does not establish the same interactions in tumors. Clinical studies also varied in disease setting, treatment combinations and endpoint definitions; consequently, single-arm activity and randomized treatment effects were considered separately. The synthesis identifies relationships supported within their experimental contexts, while the prevalence and therapeutic importance of many interactions across human cancers remain unresolved.

Conclusions

Stromal signals influence where Tregs accumulate and how they function within tumors. Tregs, in turn, can alter fibroblast and endothelial states. The clearest tumor-mechanistic examples involve CAF-dependent recruitment and antigen-dependent Treg responses, endothelial control of lymphocyte access, and feedback from Tregs to the surrounding stroma. Findings involving adipocytes and MSCs extend this picture, although their effects vary with cellular origin and tumor setting. Together, these studies show why the cells involved and their location matter when interpreting a proposed stromal-Treg interaction.

Clinical studies have not consistently translated pathway engagement into better outcomes. The next step is

to identify the interacting cells in patient tumors, determine whether treatment changes their relationship in paired tissue samples, and test whether that change improves clinical outcomes in comparative trials. This would allow stromal and immune interventions to be evaluated against a defined tumor mechanism and a measurable treatment effect.

Appendices

Appendix A: Search strategy and literature selection

Information Sources and Search Scope

A targeted PubMed update was carried out during revision on November 6, 2026. Four searches combined regulatory T-cell and cancer terms with terms for cancer-associated fibroblasts, endothelial or lymphatic cells, adipocytes, and mesenchymal stromal cells. A publication-date filter from January 1, 2023 to November 6, 2026 was applied. The update supplemented the existing reference base; older studies were retained when they provided pivotal mechanistic or clinical evidence. Publisher records and original reports were consulted to check central claims and bibliographic details.

Search topic	Hits	Retrieved
Cancer-associated fibroblasts	321	60
Endothelial and lymphatic cells	275	60
Adipocytes	42	42
Mesenchymal stromal cells	73	60

TABLE 4: Retrieval record

Results were sorted by relevance. Up to 60 records were retrieved per query. The recorded searches yielded 222 retrieved records and 210 distinct PubMed identifiers after deduplication. These are retrieval counts, not the numbers of studies included in a systematic review.

Scope and Selection Criteria

Selection was purposive and focused on stromal identity, the source and recipient of a signal, experimental perturbation, and a relevant Treg or stromal endpoint. Human tumor studies, tumor-bearing animal models and tumor-associated co-cultures were considered across cancer types. Noncancer studies were retained when they clarified a specific mechanism and were identified by their experimental setting. Reviews provided context and helped identify original reports. Clinical studies were selected for their relevance to the therapeutic pathways discussed, with attention to study design and the distinction between target engagement and treatment benefit.

Recent publications were prioritized to reflect current mechanistic and therapeutic work. Publication age alone did not determine inclusion: older original studies were retained when they established a mechanism or reported a pivotal trial. Generic associations or effects on other immune populations were not treated as direct evidence of a stromal-Treg interaction.

Selection and Source Checking

Candidate titles and selected abstracts or original reports informed the update. AI-assisted retrieval and citation cross-checking supported the process. Independent duplicate screening and formal study-level risk-of-bias assessment were not performed. The author or authors responsible for literature selection, information extraction and final source checking were: _Yang Pan and Tao Lu_.

Full PubMed search strings

All four strings below reproduce the recorded revision-stage searches performed on November 6, 2026. Search limits, ordering and retrieval counts are described on the preceding page. The retrieval limit applied to each query means the update was targeted rather than exhaustive.

Search 1: Cancer-Associated Fibroblasts

("T-Lymphocytes, Regulatory"[MeSH Terms] OR "regulatory T cells"[Title/Abstract] OR Treg*[Title/Abstract]) AND ("Neoplasms"[MeSH Terms] OR tumor*[Title/Abstract] OR tumour*[Title/Abstract] OR cancer*[Title/Abstract]) AND ("cancer-associated fibroblast*"[Title/Abstract] OR "cancer associated fibroblast*"

[Title/Abstract] OR CAFs[Title/Abstract]) AND ("2023/01/01"[Date - Publication] : "2026/11/06"[Date - Publication])

Recorded results: 321 hits; 60 records retrieved; relevance ordering.

Search 2: Endothelial and Lymphatic Cells

("T-Lymphocytes, Regulatory"[MeSH Terms] OR "regulatory T cells"[Title/Abstract] OR Treg*[Title/Abstract]) AND ("Neoplasms"[MeSH Terms] OR tumor*[Title/Abstract] OR tumour*[Title/Abstract] OR cancer*[Title/Abstract]) AND (endotheli*[Title/Abstract] OR lymphatic*[Title/Abstract]) AND ("2023/01/01"[Date - Publication] : "2026/11/06"[Date - Publication])

Recorded results: 275 hits; 60 records retrieved; relevance ordering.

Search 3: Adipocytes

("T-Lymphocytes, Regulatory"[MeSH Terms] OR "regulatory T cells"[Title/Abstract] OR Treg*[Title/Abstract]) AND ("Neoplasms"[MeSH Terms] OR tumor*[Title/Abstract] OR tumour*[Title/Abstract] OR cancer*[Title/Abstract]) AND (adipocyt*[Title/Abstract] OR "adipose tissue"[Title/Abstract]) AND ("2023/01/01"[Date - Publication] : "2026/11/06"[Date - Publication])

Recorded results: 42 hits; 42 records retrieved; relevance ordering.

Search 4: Mesenchymal Stromal Cells

("T-Lymphocytes, Regulatory"[MeSH Terms] OR "regulatory T cells"[Title/Abstract] OR Treg*[Title/Abstract]) AND ("Neoplasms"[MeSH Terms] OR tumor*[Title/Abstract] OR tumour*[Title/Abstract] OR cancer*[Title/Abstract]) AND ("mesenchymal stromal cell*"[Title/Abstract] OR "mesenchymal stem cell*"[Title/Abstract]) AND ("2023/01/01"[Date - Publication] : "2026/11/06"[Date - Publication])

Recorded results: 73 hits; 60 records retrieved; relevance ordering.

Appendix B: Evidence classification and synthesis

Evidence category	Decision rule	Interpretive scope
Direct tumor-mechanistic evidence	Identifiable source and recipient cells, a relevant perturbation in a tumor-bearing model, and a Treg-related or stromal functional endpoint. Cell-specific interventions or source-specific manipulation strengthen attribution.	Supports the tested direction and function in the specified tumor model. Broad drug exposure or depletion can leave contributions from other cells unresolved.
Tumor-associated or indirect evidence	Human tumor associations, spatial proximity, ligand–receptor inference, defined tumor-associated co-cultures, or tumor interventions that do not isolate the proposed source–recipient mechanism in vivo.	Supports an association, a cellular effect, or a plausible mechanism within the tested system. It does not by itself establish the complete interaction in an intact tumor.
Noncancer mechanistic evidence	A functional mechanism demonstrated in physiological tissue, metabolic or inflammatory disease, transplantation, or another setting without a tumor.	Provides biological context and a rationale for tumor-specific testing. Its setting remains explicit in the text and Table 1.
Hypothesis	A proposed connection assembled from separate observations or a pathway for which the relevant source, recipient, direction or functional effect has not been tested.	Identifies a testable explanation or research question. It is not presented as an established mechanism.

TABLE 5: Unit of interpretation

Evidence categories apply to the individual interaction or claim, rather than to an entire stromal population or paper. A report can support one claim directly while providing only associative evidence for another. The categories describe experimental setting and directness of mechanistic support; they are not formal certainty grades or risk-of-bias scores.

Decision Rules for Borderline Claims

An in vivo intervention was assigned direct mechanistic support only to the extent that it addressed the

stated cellular relationship and endpoint. Changes in Treg abundance alone do not establish altered suppressive function. Spatial proximity and inferred ligand-receptor pairs were interpreted as associations unless supported by functional experiments. Evidence for one signaling direction does not establish reciprocity; a reciprocal circuit requires support for both directions. Relative Treg enrichment caused by effector-cell exclusion or elimination was distinguished from an absolute increase in Treg number.

Human pharmacodynamic observations were described separately from model-based mechanisms. A change in circulating Tregs was not treated as proof of intratumoral circuit disruption without paired tumor measurements or another relevant tissue endpoint. The same distinctions were applied when interpreting the schematic arrows in the figures.

Appraisal and synthesis procedures

Study Appraisal and Conflicting Results

Appraisal considered the basis for cell identification, specificity of the perturbation, relevant controls, the functional endpoint and the model in which the result was obtained. For co-cultures, attention was given to cell preparation, culture conditions and whether other cellular sources could contribute to the effect. For human associations, attention was given to the tissue setting, sampling and whether the analysis supported a mechanistic conclusion. No formal instrument such as SYRCLE, RoB 2 or GRADE was applied, and no numerical study-quality score was assigned.

Results that differed across studies were interpreted in relation to tumor type and stage, stromal source and state, Treg phenotype, species, intervention timing and measured endpoint. Such findings were retained with their experimental context where they affected the interpretation. Evidence from distinct settings was not combined into a single universal mechanism. Functional perturbation was used to assess a proposed direction of signaling; human tissue findings informed its relevance and distribution.

Qualitative Mechanisms and Quantitative Clinical Evidence

Mechanistic findings were synthesized qualitatively around spatial positioning, functional programming, metabolic conditioning and reciprocal stromal remodeling. Clinical findings were considered within each study, recording its design, patient population, treatment regimen, analysis population and endpoint. Pharmacodynamic changes, response rates from single-arm studies and comparative efficacy from randomized trials were interpreted separately. Response percentages from different studies were not used as comparative treatment effects.

Clinical summaries retain the reported denominator and uncertainty relevant to the conclusion. Objective response rates are accompanied by the response-analysis population and reported confidence interval where available. Randomized comparisons are described using the reported effect estimate and confidence interval, with the relevant endpoint and statistical result. Safety comparisons retain event counts, denominators and the definition of the adverse-event category. Where the original reports did not provide these estimates, 95% confidence intervals for the expanded COMBAT response proportions were derived from published counts using the Clopper-Pearson method, and the bintrafusp alfa severe-toxicity risk difference and its 95% confidence interval were derived using the Newcombe method. These estimates are identified in Tables *2*-*3*. Values not reported in the original source are identified rather than inferred from rounded percentages. No pooled effect estimate, meta-analysis or meta-regression was undertaken.

AI Assistance and Verification

OpenAI Codex assisted the revision-stage search, bibliographic cross-checking and organization. Recorded search strings and retrieval counts were retained. Bibliographic checks compared titles, authors, publication details and DOI or publisher links with source records. Central mechanistic and clinical claims were checked against the relevant source material where available; an abstract or metadata record alone was not treated as confirmation of every experimental detail. The authors are responsible for final source selection, interpretation and verification. No independent duplicate human screening or formal bias assessment is implied by the use of AI tools.

The main AI-use disclosure remains in the manuscript disclosures. Figures *1*-*3* were drawn by Yang Pan using BioRender, with its drawing tools and supplied assets; no generative AI images or icons were used.

Appendix C: SANRA informed reporting self-check

SANRA domain	Manuscript location	Reporting focus
Importance of the review	Introduction and Background	The role of Tregs in immune regulation and tumor immune suppression, and the clinical relevance of stromal interactions to immune exclusion and treatment response.
Specific aims	Final introductory paragraph	Comparison of Treg interactions across CAFs, blood and lymphatic endothelial cells, adipocytes and MSCs through four organizing processes, with therapeutic implications.
Literature search	Literature selection and evidence appraisal; Appendix A	Actual revision-stage search date, database, complete search strings, date filter, retrieval limit and counts, purposive selection, and screening responsibilities.
Referencing	Mechanistic and clinical sections; Tables 1-3; Appendix B	Citations matched to the specific claim, original studies used for central mechanisms and trial outcomes, and bibliographic and DOI or publisher-link checks.
Scientific reasoning	Mechanistic sections; Tables 2-3; Appendix B	Claim-level categories based on setting and experimental directness, separation of association from functional perturbation, and interpretation of discordant results by model and cellular context.
Presentation of endpoint data	Clinical translation section; Table 2; Appendix B	Study design, analysis populations, relevant effect estimates, reported or explicitly derived confidence intervals and safety denominators; distinction between pharmacodynamic findings, single-arm activity and randomized comparisons.

TABLE 6: SANRA informed reporting self check

The six SANRA domains are used here to organize a reporting self-check and identify where the relevant information belongs in the review. No numerical SANRA score was assigned. This map assesses reporting of the narrative review and is not a study-level risk-of-bias assessment.

Abbreviations: CAF, cancer-associated fibroblast; DOI, digital object identifier; GRADE, Grading of Recommendations Assessment, Development and Evaluation; MSC, mesenchymal stromal cell; RoB 2, revised Cochrane risk-of-bias tool for randomized trials; SANRA, Scale for the Assessment of Narrative Review Articles; SYRCLE, Systematic Review Centre for Laboratory animal Experimentation; Treg, regulatory T cell.

Additional Information

Author Contributions

All authors have reviewed the final version to be published and agreed to be accountable for all aspects of the work.

Concept and design: Yang Pan, Tao Lu, Xixian Ke, Junliang Ma

Acquisition, analysis, or interpretation of data: Yang Pan, Tao Lu, Jiajie Wang, Bingbing Lu

Drafting of the manuscript: Yang Pan, Tao Lu

Critical review of the manuscript for important intellectual content: Yang Pan, Tao Lu, Jiajie Wang, Bingbing Lu, Xixian Ke, Junliang Ma

Supervision: Xixian Ke, Junliang Ma

Disclosures

Conflicts of interest: In compliance with the ICMJE uniform disclosure form, all authors declare the following: **Payment/services info:** This work was supported by the National Natural Science Foundation of China (Grant No. 82260550). **Financial relationships:** All authors have declared that they have no financial relationships at present or within the previous three years with any organizations that might have an interest in the submitted work. **Other relationships:** All authors have declared that there are no other relationships or activities that could appear to have influenced the submitted work.

Acknowledgements

We thank OpenAI for providing Codex, which was used to assist with reference checking and manuscript organization. The authors retain full responsibility for the selection and critical appraisal of the literature,

verification of references, accuracy of the scientific content, and all interpretations and conclusions in the final manuscript. We thank BioRender for providing the illustration tools and graphical resources used to create Figures 1-3.

References

1. de Visser KE, Joyce JA: The evolving tumor microenvironment: from cancer initiation to metastatic outgrowth. Cancer Cell. 2023, 41:374-403. 10.1016/j.ccell.2023.02.016
2. Imianowski CJ, Chen Q, Workman CJ, Vignali DA: Regulatory T cells in the tumour microenvironment . Nat Rev Cancer. 2025, 25:703-22. 10.1038/s41568-025-00832-9
3. Wang L, Liang Y, Zhao C, et al.: Regulatory T cells in homeostasis and disease: molecular mechanisms and therapeutic potential. Signal Transduct Target Ther. 2025, 10:345. 10.1038/s41392-025-02326-4
4. Jia H, Chen X, Zhang L, Chen M: Cancer associated fibroblasts in cancer development and therapy . J Hematol Oncol. 2025, 18:36. 10.1186/s13045-025-01688-0
5. Arpinati L, Carradori G, Scherz-Shouval R: CAF-induced physical constraints controlling T cell state and localization in solid tumours. Nat Rev Cancer. 2024, 24:676-93. 10.1038/s41568-024-00740-4
6. Piao W, Lee ZL, Zapas G, Wu L, Jewell CM, Abdi R, Bromberg JS: Regulatory T cell and endothelial cell crosstalk. Nat Rev Immunol. 2025, 25:588-607. 10.1038/s41577-025-01149-2
7. Lanitis E, Irving M, Coukos G: Tumour-associated vasculature in T cell homing and immunity: opportunities for cancer therapy. Nat Rev Immunol. 2025, 25:831-46. 10.1038/s41577-025-01187-w
8. Watts EL, Gonzalez-Feliciano A, Gunter MJ, Chatterjee N, Moore SC: Adiposity and cancer: epidemiology, mechanisms and future perspectives. Nat Metab. 2026, 8:1266-81. 10.1038/s42255-026-01529-5
9. Zhang Y, Wang C, Li JJ: Revisiting the role of mesenchymal stromal cells in cancer initiation, metastasis and immunosuppression. Exp Hematol Oncol. 2024, 13:64. 10.1186/s40164-024-00532-4
10. Tang J, Chen Y, Wang C, et al.: The role of mesenchymal stem cells in cancer and prospects for their use in cancer therapeutics. MedComm (2020). 2024, 5:e663. 10.1002/mco2.663
11. Cords L, de Souza N, Bodenmiller B: Classifying cancer-associated fibroblasts-The good, the bad, and the target. Cancer Cell. 2024, 42:1480-5. 10.1016/j.ccell.2024.08.011
12. Liu Y, Chen X, Dai Y, et al.: Molecular phenotypes and spatial archetypes: a new framework for cancer-associated fibroblasts. Cancer Cell. 2026, 44:1346-67. 10.1016/j.ccell.2026.06.001
13. Feig C, Jones JO, Kraman M, et al.: Targeting CXCL12 from FAP-expressing carcinoma-associated fibroblasts synergizes with anti-PD-L1 immunotherapy in pancreatic cancer. Proc Natl Acad Sci U S A. 2013, 110:20212-7. 10.1073/pnas.1320318110
14. Biasci D, Smoragiewicz M, Connell CM, et al.: CXCR4 inhibition in human pancreatic and colorectal cancers induces an integrated immune response. Proc Natl Acad Sci U S A. 2020, 117:28960-70. 10.1073/pnas.2013644117
15. Huang YH, Chang CY, Kuo YZ, Fang WY, Kao HY, Tsai ST, Wu LW: Cancer-associated fibroblast-derived interleukin-1β activates protumor C-C motif chemokine ligand 22 signaling in head and neck cancer. Cancer Sci. 2019, 110:2783-93. 10.1111/cas.14135
16. Huang H, Wang Z, Zhang Y, et al.: Mesothelial cell-derived antigen-presenting cancer-associated fibroblasts induce expansion of regulatory T cells in pancreatic cancer. Cancer Cell. 2022, 40:656-73. 10.1016/j.ccell.2022.04.011
17. Varveri A, Papadopoulou M, Papadovasilakis Z, et al.: Immunological synapse formation between T regulatory cells and cancer-associated fibroblasts promotes tumour development. Nat Commun. 2024, 15:4988. 10.1038/s41467-024-49282-1
18. Sun R, Zhao H, Gao DS, et al.: Amphiregulin couples IL1RL1(+) regulatory T cells and cancer-associated fibroblasts to impede antitumor immunity. Sci Adv. 2023, 9:eadd7399. 10.1126/sciadv.add7399
19. Nummer D, Suri-Payer E, Schmitz-Winnenthal H, et al.: Role of tumor endothelium in CD4+ CD25+ regulatory T cell infiltration of human pancreatic carcinoma. J Natl Cancer Inst. 2007, 99:1188-99. 10.1093/jnci/djm064
20. Motz GT, Santoro SP, Wang LP, et al.: Tumor endothelium FasL establishes a selective immune barrier promoting tolerance in tumors. Nat Med. 2014, 20:607-15. 10.1038/nm.3541
21. Zhang L, Xu J, Zhou S, et al.: Endothelial DGKG promotes tumor angiogenesis and immune evasion in hepatocellular carcinoma. J Hepatol. 2024, 80:82-98. 10.1016/j.jhep.2023.10.006
22. Akeus P, Szeponik L, Ahlmanner F, et al.: Regulatory T cells control endothelial chemokine production and migration of T cells into intestinal tumors of APC(min/+) mice. Cancer Immunol Immunother. 2018, 67:1067-77. 10.1007/s00262-018-2161-9
23. Akeus P, Szeponik L, Langenes V, et al.: Regulatory T cells reduce endothelial neutral sphingomyelinase 2 to prevent T-cell migration into tumors. Eur J Immunol. 2021, 51:2317-29. 10.1002/eji.202149208
24. Piao W, Wu L, Xiong Y, et al.: Regulatory T cells crosstalk with tumor cells and endothelium through lymphotoxin signaling. Nat Commun. 2024, 15:10468. 10.1038/s41467-024-54874-y
25. Wang C, Zhang X, Luo L, et al.: Adipocyte-derived PGE2 is required for intermittent fasting-induced Treg proliferation and improvement of insulin sensitivity. JCI Insight. 2022, 7:153755. 10.1172/jci.insight.153755
26. Zhu Q, Cao Y, Yuan J, Hu Y: Adipose-derived stem cell exosomes promote tumor characterization and immunosuppressive microenvironment in breast cancer. Cancer Immunol Immunother. 2024, 73:39. 10.1007/s00262-023-03584-3
27. Patel SA, Meyer JR, Greco SJ, Corcoran KE, Bryan M, Rameshwar P: Mesenchymal stem cells protect breast cancer cells through regulatory T cells: role of mesenchymal stem cell-derived TGF-beta. J Immunol. 2010, 184:5885-94. 10.4049/jimmunol.0903143
28. Wu L, Lin Q, Ma Z, Chowdhury FA, Mazumder MH, Du W: Mesenchymal PGD(2) activates an ILC2-Treg axis to promote proliferation of normal and malignant HSPCs. Leukemia. 2020, 34:3028-41. 10.1038/s41375-020-0843-8
29. Tang RJ, Shen SN, Zhao XY, et al.: Mesenchymal stem cells-regulated Treg cells suppress colitis-associated colorectal cancer. Stem Cell Res Ther. 2015, 6:71. 10.1186/s13287-015-0055-8

30. François S, Usunier B, Forgue-Lafitte ME, et al.: Mesenchymal stem cell administration attenuates colon cancer progression by modulating the Immune component within the colorectal tumor microenvironment. Stem Cells Transl Med. 2019, 8:285-300. 10.1002/sctm.18-0117
31. Mariathasan S, Turley SJ, Nickles D, et al.: TGFβ attenuates tumour response to PD-L1 blockade by contributing to exclusion of T cells. Nature. 2018, 554:544-8. 10.1038/nature25501
32. Cheng JT, Deng YN, Yi HM, et al.: Hepatic carcinoma-associated fibroblasts induce IDO-producing regulatory dendritic cells through IL-6-mediated STAT3 activation. Oncogenesis. 2016, 5:e198. 10.1038/oncsis.2016.7
33. Zhao Y, Sun J, Liang Y, et al.: Increased expression of ST2 on regulatory T cells is associated with cancer associated fibroblast-derived IL-33 in laryngeal cancer. Pathol Res Pract. 2022, 237:154023. 10.1016/j.prp.2022.154023
34. Cao Z, Meng Z, Li J, et al.: Interferon-γ-stimulated antigen-presenting cancer-associated fibroblasts hinder neoadjuvant chemoimmunotherapy efficacy in lung cancer. Cell Rep Med. 2025, 6:102017. 10.1016/j.xcrm.2025.102017
35. Croizer H, Mhaidly R, Kieffer Y, et al.: Deciphering the spatial landscape and plasticity of immunosuppressive fibroblasts in breast cancer. Nat Commun. 2024, 15:2806. 10.1038/s41467-024-47068-z
36. Watson MJ, Vignali PD, Mullett SJ, et al.: Metabolic support of tumour-infiltrating regulatory T cells by lactic acid. Nature. 2021, 591:645-51. 10.1038/s41586-020-03045-2
37. Kumagai S, Koyama S, Itahashi K, et al.: Lactic acid promotes PD-1 expression in regulatory T cells in highly glycolytic tumor microenvironments. Cancer Cell. 2022, 40:201-18. 10.1016/j.ccell.2022.01.001
38. Ding R, Yu X, Hu Z, et al.: Lactate modulates RNA splicing to promote CTLA-4 expression in tumor-infiltrating regulatory T cells. Immunity. 2024, 57:528-40. 10.1016/j.immuni.2024.01.019
39. Kim TH, Lim SH, Lee H, Chae YC, Min DS: Metabolic crosstalk among cancer-associated fibroblasts, adipocytes and immune cells as an immunosuppressive tumor microenvironment driver. Exp Mol Med. 2026, 58:366-81. 10.1038/s12276-026-01650-1
40. Ye L, Xiang X, Wang Z, et al.: H3K18 lactylation in cancer-associated fibroblasts drives malignant pleural effusion progression via TNFR2(+) T(reg) recruitment. Exp Mol Med. 2025, 57:2671-85. 10.1038/s12276-025-01557-3
41. Mezrich JD, Fechner JH, Zhang X, Johnson BP, Burlingham WJ, Bradfield CA: An interaction between kynurenine and the aryl hydrocarbon receptor can generate regulatory T cells. J Immunol. 2010, 185:3190-8. 10.4049/jimmunol.0903670
42. Solvay M, Holfelder P, Klaessens S, et al.: Tryptophan depletion sensitizes the AHR pathway by increasing AHR expression and GCN2/LAT1-mediated kynurenine uptake, and potentiates induction of regulatory T lymphocytes. J Immunother Cancer. 2023, 11:6728. 10.1136/jitc-2023-006728
43. Hu Y, Liang J, Duan L, et al.: Cytokines and cancer-associated fibroblasts . J Hematol Oncol. 2026, 19:43. 10.1186/s13045-026-01801-x
44. Prawira A, Xu H, Mei Y, et al.: Targeting Treg-fibroblast interaction to enhance immunotherapy in steatotic liver disease-related hepatocellular carcinoma. Gut. 2025, 75:105-18. 10.1136/gutjnl-2025-335084
45. Heide J, Bilecz AJ, Patnaik S, et al.: NNMT inhibition in cancer-associated fibroblasts restores antitumour immunity. Nature. 2025, 645:1051-9. 10.1038/s41586-025-09303-5
46. Carambia A, Freund B, Schwinge D, et al.: TGF-β-dependent induction of $CD4^+CD25^+Foxp3^+$ Tregs by liver sinusoidal endothelial cells. J Hepatol. 2014, 61:594-9. 10.1016/j.jhep.2014.04.027
47. Oettel A, Lorenz M, Stangl V, Costa SD, Zenclussen AC, Schumacher A: Human umbilical vein endothelial cells foster conversion of CD4+CD25-Foxp3- T cells into CD4+Foxp3+ regulatory T cells via transforming growth factor-β. Sci Rep. 2016, 6:23278. 10.1038/srep23278
48. Shetty S, Weston CJ, Oo YH, et al.: Common lymphatic endothelial and vascular endothelial receptor-1 mediates the transmigration of regulatory T cells across human hepatic sinusoidal endothelium. J Immunol. 2011, 186:4147-55. 10.4049/jimmunol.1002961
49. Fu H, Kishore M, Gittens B, et al.: Self-recognition of the endothelium enables regulatory T-cell trafficking and defines the kinetics of immune regulation. Nat Commun. 2014, 5:3436. 10.1038/ncomms4436
50. Piao W, Li L, Saxena V, et al.: PD-L1 signaling selectively regulates T cell lymphatic transendothelial migration. Nat Commun. 2022, 13:2176. 10.1038/s41467-022-29930-0
51. Flati V, Pastore LI, Griffioen AW, et al.: Endothelial cell anergy is mediated by bFGF through the sustained activation of p38-MAPK and NF-kappaB inhibition. Int J Immunopathol Pharmacol. 2006, 19:761-73. 10.1177/039463200601900406
52. Hellebrekers DM, Castermans K, Viré E, et al.: Epigenetic regulation of tumor endothelial cell anergy: silencing of intercellular adhesion molecule-1 by histone modifications. Cancer Res. 2006, 66:10770-7. 10.1158/0008-5472.CAN-06-1609
53. Delfortrie S, Pinte S, Mattot V, et al.: Egfl7 promotes tumor escape from immunity by repressing endothelial cell activation. Cancer Res. 2011, 71:7176-86. 10.1158/0008-5472.CAN-11-1301
54. Buckanovich RJ, Facciabene A, Kim S, et al.: Endothelin B receptor mediates the endothelial barrier to T cell homing to tumors and disables immune therapy. Nat Med. 2008, 14:28-36. 10.1038/nm1699
55. Lu Y, Liu Y, Zuo X, et al.: CXCL12(+) tumor-associated endothelial cells promote immune resistance in hepatocellular carcinoma. J Hepatol. 2025, 82:634-48. 10.1016/j.jhep.2024.09.044
56. Wang Y, Chen Y, Liu Y, et al.: Tumor vascular endothelial cells promote immune escape by upregulating PD-L1 expression via crosstalk between NF-κB and STAT3 signaling pathways in nasopharyngeal carcinoma. Cell Death Dis. 2025, 16:129. 10.1038/s41419-025-07444-z
57. Georganaki M, Ramachandran M, Tuit S, et al.: Tumor endothelial cell up-regulation of IDO1 is an immunosuppressive feed-back mechanism that reduces the response to CD40-stimulating immunotherapy. Oncoimmunology. 2020, 9:1730538. 10.1080/2162402X.2020.1730538
58. Wang L, Fan J, Thompson LF, Zhang Y, Shin T, Curiel TJ, Zhang B: CD73 has distinct roles in nonhematopoietic and hematopoietic cells to promote tumor growth in mice. J Clin Invest. 2011, 121:2371-82. 10.1172/JCI45559
59. Kabir AU, Subramanian M, Kwon Y, Choi K: Linking tumour angiogenesis and tumour immunity. Nat Rev

Immunol. 2026, 26:35-51. 10.1038/s41577-025-01211-z
60. Kuo HY, Khan KA, Kerbel RS: Antiangiogenic-immune-checkpoint inhibitor combinations: lessons from phase III clinical trials. Nat Rev Clin Oncol. 2024, 21:468-82. 10.1038/s41571-024-00886-y
61. Facciabene A, Peng X, Hagemann IS, et al.: Tumour hypoxia promotes tolerance and angiogenesis via CCL28 and T(reg) cells. Nature. 2011, 475:226-30. 10.1038/nature10169
62. Cipolletta D, Feuerer M, Li A, et al.: PPAR-γ is a major driver of the accumulation and phenotype of adipose tissue Treg cells. Nature. 2012, 486:549-53. 10.1038/nature11132
63. Elkins C, Li C: Deciphering visceral adipose tissue regulatory T cells: key contributors to metabolic health . Immunol Rev. 2024, 324:52-67. 10.1111/imr.13336
64. De Rosa V, Procaccini C, Calì G, et al.: A key role of leptin in the control of regulatory T cell proliferation . Immunity. 2007, 26:241-55. 10.1016/j.immuni.2007.01.011
65. Kälin S, Becker M, Ott VB, et al.: A Stat6/Pten axis links regulatory T cells with adipose tissue function . Cell Metab. 2017, 26:475-92. 10.1016/j.cmet.2017.08.008
66. Nikolic I, Ruiz-Garrido I, Crespo M, et al.: Lack of p38 activation in T cells increases IL-35 and protects against obesity by promoting thermogenesis. EMBO Rep. 2024, 25:2635-61. 10.1038/s44319-024-00149-y
67. Wang G, Muñoz-Rojas AR, Spallanzani RG, Franklin RA, Benoist C, Mathis D: Adipose-tissue Treg cells restrain differentiation of stromal adipocyte precursors to promote insulin sensitivity and metabolic homeostasis. Immunity. 2024, 57:1345-59. 10.1016/j.immuni.2024.04.002
68. Beppu LY, Mooli RG, Qu X, et al.: Tregs facilitate obesity and insulin resistance via a Blimp-1/IL-10 axis . JCI Insight. 2021, 6:140644. 10.1172/jci.insight.140644
69. Liu M, Starenki D, Scharer CD, et al.: Circulating Tregs accumulate in omental tumors and acquire adipose-resident features. Cancer Immunol Res. 2022, 10:641-55. 10.1158/2326-6066.CIR-21-0880
70. Wang H, Franco F, Tsui YC, et al.: CD36-mediated metabolic adaptation supports regulatory T cell survival and function in tumors. Nat Immunol. 2020, 21:298-308. 10.1038/s41590-019-0589-5
71. Giannitti G, Kamińska K, Marchesi S, Garavaglia R, Preosto I, Grzesiak M, Fontana F: Extracellular vesicles released from prostate cancer cells confer pro-tumor properties to adipocytes by stimulating lipolysis. Biofactors. 2025, 51:e70067. 10.1002/biof.70067
72. Dai W, Luo W, Fang H, et al.: Cancer-associated adipocytes promote peritoneal metastasis of colorectal signet ring cell carcinoma via FABP4 induction. Cell Commun Signal. 2025, 24:29. 10.1186/s12964-025-02569-2
73. Tong Y, Wang Z, Qiao N, et al.: Decoding adipocyte heterogeneity through single-nucleus transcriptomics unveils subtype-specific adipocytes orchestrate immunosuppressive niches in breast cancer. J Immunother Cancer. 2026, 14:12711. 10.1136/jitc-2025-012711
74. Hu X, Jia F, Li L, et al.: Single-cell and single-nuclei transcriptomics profiling reveals dynamic cellular features in tumor-related adipose microenvironment of breast cancer patients with high BMI. Transl Oncol. 2025, 57:102408. 10.1016/j.tranon.2025.102408
75. Wang Q, Guo W, Niu L, et al.: 3D-hUMSCs exosomes ameliorate vitiligo by simultaneously potentiating Treg cells-mediated immunosuppression and suppressing oxidative stress-induced melanocyte damage. Adv Sci (Weinh). 2024, 11:e2404064. 10.1002/advs.202404064
76. Chen J, Shi X, Deng Y, et al.: miRNA-148a-containing GMSC-derived EVs modulate Treg/Th17 balance via IKKB/NF-κB pathway and treat a rheumatoid arthritis model. JCI Insight. 2024, 9:177841. 10.1172/jci.insight.177841
77. Ji J, Liang Q, He Q, et al.: Overexpression of miR-20a-5p in mesenchymal stem cell derived-exosomes from systemic lupus erythematosus patients restored therapeutic effect and Treg immune regulation. Eur J Pharmacol. 2024, 979:176862. 10.1016/j.ejphar.2024.176862
78. Lee HJ, Choi YR, Ko JH, Ryu JS, Oh JY: Defining mesenchymal stem/stromal cell-induced myeloid-derived suppressor cells using single-cell transcriptomics. Mol Ther. 2024, 32:1970-83. 10.1016/j.ymthe.2024.04.026
79. Mittal SK, Cho W, Elbasiony E, Guan Y, Foulsham W, Chauhan SK: Mesenchymal stem cells augment regulatory T cell function via CD80-mediated interactions and promote allograft survival. Am J Transplant. 2022, 22:1564-77. 10.1111/ajt.17001
80. Sirpilla O, Sakemura RL, Hefazi M, et al.: Mesenchymal stromal cells with chimaeric antigen receptors for enhanced immunosuppression. Nat Biomed Eng. 2024, 8:443-60. 10.1038/s41551-024-01195-6
81. Bautista-Sebastián E, Cortés-Morales VA, Fajardo-Orduña GR, et al.: Interaction between mesenchymal stromal cells and tumor cells present in cervical cancer influences macrophage polarization. Cancers (Basel). 2025, 17:3099. 10.3390/cancers17193099
82. Ling W, Zhang J, Yuan Z, et al.: Mesenchymal stem cells use IDO to regulate immunity in tumor microenvironment. Cancer Res. 2014, 74:1576-87. 10.1158/0008-5472.CAN-13-1656
83. Zhang R, Liu Q, Zhou S, He H, Zhao M, Ma W: Mesenchymal stem cell suppresses the efficacy of CAR-T toward killing lymphoma cells by modulating the microenvironment through stanniocalcin-1. Elife. 2023, 12:82934. 10.7554/eLife.82934
84. Hu W, Wang W, Jiang X, Wang Z, Lin R: Mesenchymal stem cells can prevent or promote the progression of colon cancer based on their timing of administration. J Transl Med. 2023, 21:227. 10.1186/s12967-023-04028-3
85. Jenkins BH, Tracy I, Rodrigues MF, et al.: Single cell and spatial analysis of immune-hot and immune-cold tumours identifies fibroblast subtypes associated with distinct immunological niches and positive immunotherapy response. Mol Cancer. 2025, 24:3. 10.1186/s12943-024-02191-9
86. Jinushi K, Saito T, Kurose K, et al.: Phase I study on neoadjuvant combination immunotherapy with mogamulizumab and nivolumab for solid tumors. J Immunother Cancer. 2025, 13:10634. 10.1136/jitc-2024-010634
87. Aung TN, Monkman J, Warrell J, et al.: Spatial signatures for predicting immunotherapy outcomes using multi-omics in non-small cell lung cancer. Nat Genet. 2025, 57:2482-93. 10.1038/s41588-025-02351-7
88. Bockorny B, Semenisty V, Macarulla T, et al.: BL-8040, a CXCR4 antagonist, in combination with pembrolizumab and chemotherapy for pancreatic cancer: the COMBAT trial. Nat Med. 2020, 26:878-85. 10.1038/s41591-020-0880-x

89. Bockorny B, Macarulla T, Semenisty V, et al.: Motixafortide and pembrolizumab combined to nanoliposomal irinotecan, fluorouracil, and folinic acid in metastatic pancreatic cancer: the COMBAT/KEYNOTE-202 trial. Clin Cancer Res. 2021, 27:5020-7. 10.1158/1078-0432.CCR-21-0929
90. Hong DS, Rixe O, Chiu VK, et al.: Mogamulizumab in combination with nivolumab in a phase I/II study of patients with locally advanced or metastatic solid tumors. Clin Cancer Res. 2022, 28:479-88. 10.1158/1078-0432.CCR-21-2781
91. Cho BC, Lee JS, Wu YL, et al.: Bintrafusp alfa versus pembrolizumab in patients with treatment-naive, programmed death-ligand 1-high advanced NSCLC: a randomized, open-label, phase 3 trial. J Thorac Oncol. 2023, 18:1731-42. 10.1016/j.jtho.2023.08.018
92. Socinski MA, Jotte RM, Cappuzzo F, et al.: Atezolizumab for first-line treatment of metastatic nonsquamous NSCLC. N Engl J Med. 2018, 378:2288-301. 10.1056/NEJMoa1716948
93. Finn RS, Qin S, Ikeda M, et al.: Atezolizumab plus bevacizumab in unresectable hepatocellular carcinoma . N Engl J Med. 2020, 382:1894-905. 10.1056/NEJMoa1915745
94. Coveler AL, Reilley MJ, Zalupski M, et al.: A phase Ib/II randomized clinical trial of oleclumab with or without durvalumab plus chemotherapy in patients with metastatic pancreatic ductal adenocarcinoma. Clin Cancer Res. 2024, 30:4609-17. 10.1158/1078-0432.CCR-24-0499
95. Long GV, Dummer R, Hamid O, et al.: Epacadostat plus pembrolizumab versus placebo plus pembrolizumab in patients with unresectable or metastatic melanoma (ECHO- 301/KEYNOTE-252): a phase 3, randomised, double-blind study. Lancet Oncol. 2019, 20:1083-97. 10.1016/S1470-2045(19)30274-8
96. Klughammer J, Abravanel DL, Segerstolpe Å, et al.: A multi-modal single-cell and spatial expression map of metastatic breast cancer biopsies across clinicopathological features. Nat Med. 2024, 30:3236-49. 10.1038/s41591-024-03215-z
97. Raufi AG, D'Souza EK, May MS, et al.: Motixafortide, cemiplimab, gemcitabine and nab-paclitaxel in metastatic pancreatic cancer: a single-arm phase 2 study with single-cell correlatives. Nat Commun. 2026, 17:10350. 10.1038/s41467-026-76559-4